Science Signaling
AAAS

www.sciencesignaling.org/cgi/content/full/8/358/ra1/DC1

Supplementary Materials for

The kinase activity of the Ser/Thr kinase BUB1 promotes TGF-β signaling

Shyam Nyati, Katrina Schinske-Sebolt, Sethuramasundaram Pitchiaya, Katerina Chekhovskiy, Areeb Chator, Nauman Chaudhry, Joseph Dosch, Marcian E. Van Dort, Sooryanarayana Varambally, Chandan Kumar-Sinha, Mukesh Kumar Nyati, Dipankar Ray, Nils G. Walter, Hongtao Yu, Brian Dale Ross, Alnawaz Rehemtulla*

*Corresponding author. E-mail: alnawaz@med.umich.edu

Published 6 January 2015, *Sci. Signal.* **8**, ra1 (2015)
DOI: 10.1126/scisignal.2005379

This PDF file includes:

Other Supplementary Material for this manuscript includes the following:
(available at www.sciencesignaling.org/cgi/content/full/8/358/ra1/DC1)

Table S1 (Microsoft Excel format). Human kinome siRNA screen in A549-BTR and MDA-231-1833–BTR cells.
Table S2 (Microsoft Excel format). Hits obtained in A549-BTR and MDA-231-1833–BTR human kinome screen.

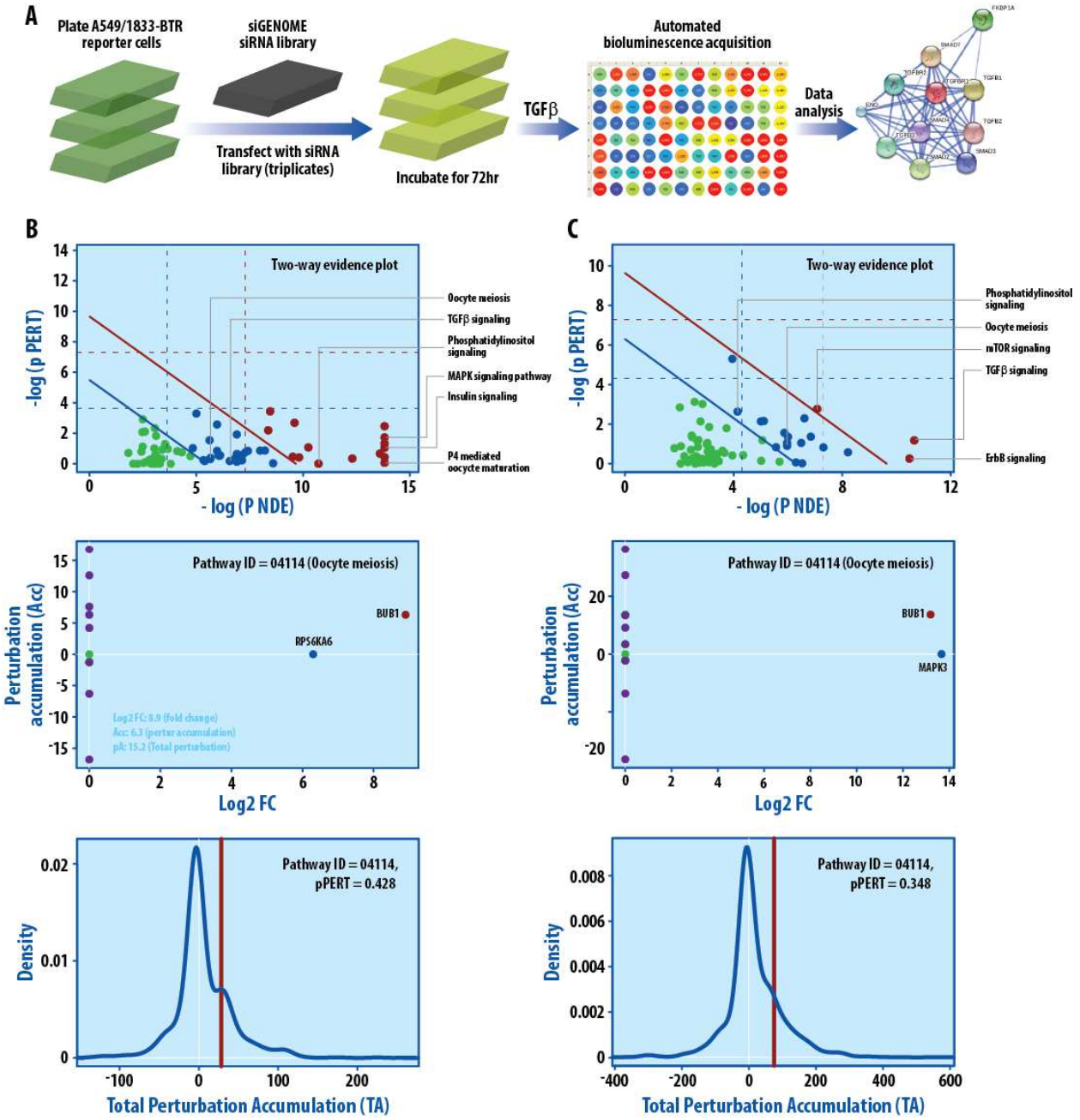

Figure S1. siRNA screening and pathway analysis. (A) Schematic representation of siRNA screening strategy. siGENOME human kinome siRNA library was transfected in reporter expressing A549-BTR and MDA-231-1833-BTR cells (in triplicates) using Dharmafect1 reagent and a Beckman Coulter Biomek liquid handling system. Cells were incubated for 60 hours after transfection, serum-starved overnight, and TGF-β (10 ng/mL) was added for 1 hour, after which reporter activity was assessed upon addition of D-Luciferin (50 µg/ml) using an InVision plate reader. **(B and C)** Two-way evidence plots of high and low stringency hits generated by Pathway-Guide (top) and perturbation accumulation analysis of a selected pathway, the oocyte meiosis pathway (middle and bottom) in A549-BTR cells (B) and MDA-231-1833-BTR cells (C). Two-way evidence plots show the hypergeometric (over-representation, P_{NDE}) vs. perturbation p-values (P_{PERT}) for all the pathways. Pathways above the oblique red line are significant at 5% after Bonferroni correction; those above the oblique blue line are significant at 5% after FDR correction. The vertical and horizontal thresholds represent the same corrections for the two types of evidence considered individually. Oocyte meiosis pathway analysis (middle) shows the highest total perturbation accumulation (pA for BUB1, red dot). X-axis is Log2 FC (fold

change; BTR fold activation), and the Y-axis is perturbation accumulation (Acc) for a given gene in the pathway. Genes (green dots) on the gray line (along the Y-axis are) are not input genes, therefore they show only perturbation accumulation but no fold change values. To better understand the perturbation p-value of this selected pathway, its total accumulation is shown on the distribution of the total accumulations under the null hypothesis (bottom).

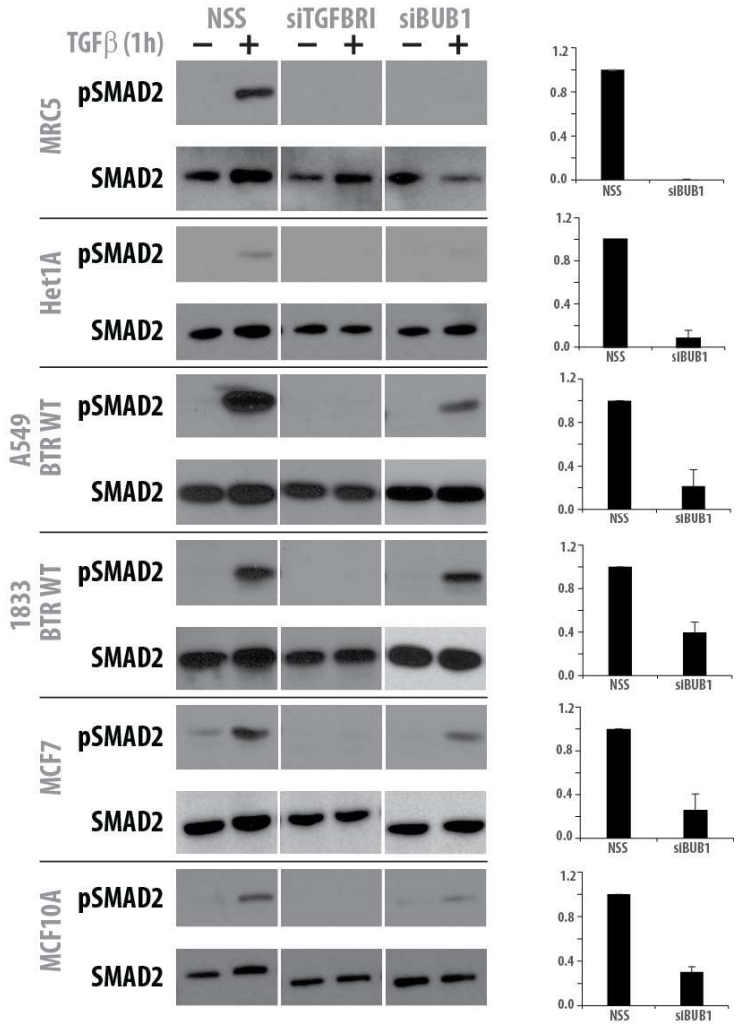

Figure S2. BUB1 mediates TGF-β–dependent SMAD2/3 phosphorylation. Lung (A549), and breast (MDA-231-1833, MCF7) cancer as well as non-tumoregenic lines (MRC5, MCF10A, Het1A) were transfected with scrambled control (NSS, negative control), TGFBRI (positive control), or BUB1 siRNA and treated with TGF-β (10 ng/mL) for an hour. Extracts were prepared and analyzed for phosphorylated SMAD2 and SMAD2 abundance by immunoblot analysis. Data are means ± SD from at least three biological replicates (TGF-β-treated samples only).

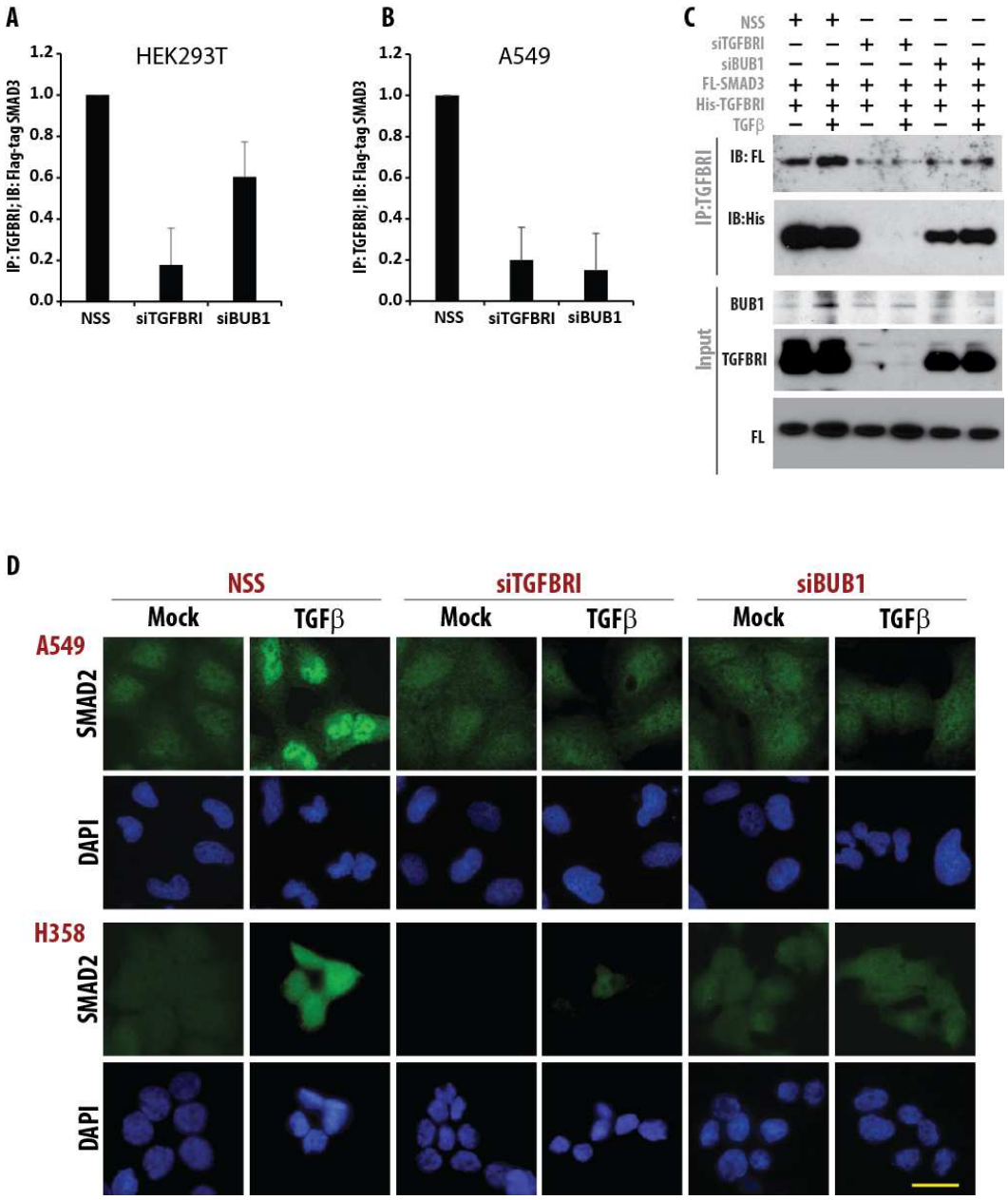

Figure S3. Depletion of BUB1 leads to reduced SMAD3 recruitment to TGFBRI and TGF-β–dependent accumulation of SMAD2 in the nucleus. (A to B). Western blot quantitation of data in Fig. 2A (HEK293T) and Fig. 2B (A549). Data are means ± SD from 3 biological replicates. **(C)** Western blot of FL-SMAD3 immunoprecipitated with TGFBRI antibody in A549 cells transfected with FL-SMAD3, His-TGFBRI and siRNA to TGFBRI or BUB1, and treated with TGF-β (10 ng/mL, 1 hour). Blots are representative of 2 independent experiments. **(D)** Immunofluorescence for SMAD2 in A549 and NCI-H358 cells transfected for 60 hours with control or TGFBRI- or BUB1-specific siRNA. Cells were serum-starved overnight and treated with TGF-β or vehicle (mock) for 1 hour. DAPI counter-stained the nuclei (blue). Scale bar, 25 μm. Images are representative of 3 independent experiments.

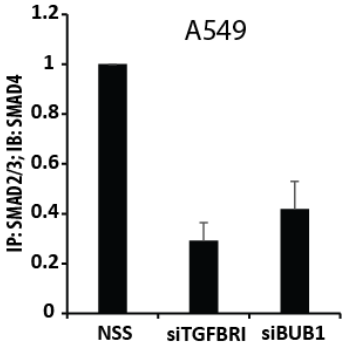

Figure S4. Depletion of BUB1 attenuates TGF-β–dependent SMAD2/3-SMAD4 complex formation in A549 cells. Quantitative analysis of immunoblot results in Fig. 2C. Data are means ± S.E.M. from 3 biological replicates.

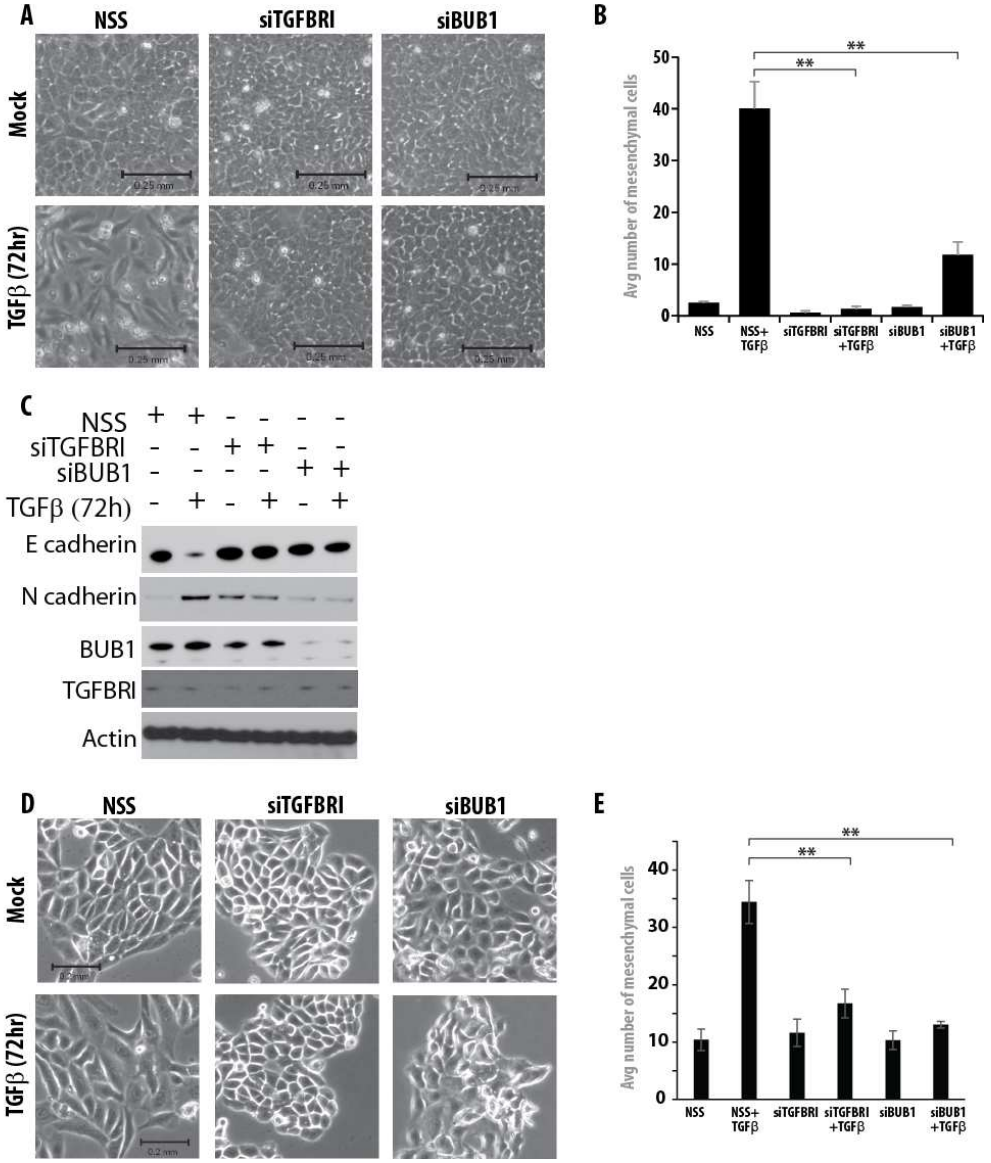

Figure S5. Depletion of BUB1 inhibits TGF-β–mediated EMT in A549 and NCI-H358 cells. Light microscopy to assess morphology of A549 (**A and B**) and NCI-H358 (**D and E**) cells transfected with control siRNA (NSS), TGFBRI siRNA, or BUB1 siRNA and either mock-treated or treated with TGF-β (10 ng/mL) for

72 hours. Images of 3 random fields for each treatment were taken at 40X objective. Data are means ± S.E.M. from 3 biological replicates. **P<0.001, two-sided Student's t-test. Scale bars, 0.25 mm (A), 0.2 mm (D). **(C)** Representative Western blots for E-Cadherin and N-Cadherin in lysates from A549 cells transfected and treated as in (A and B). Blots are representative of 3 biological replicates.

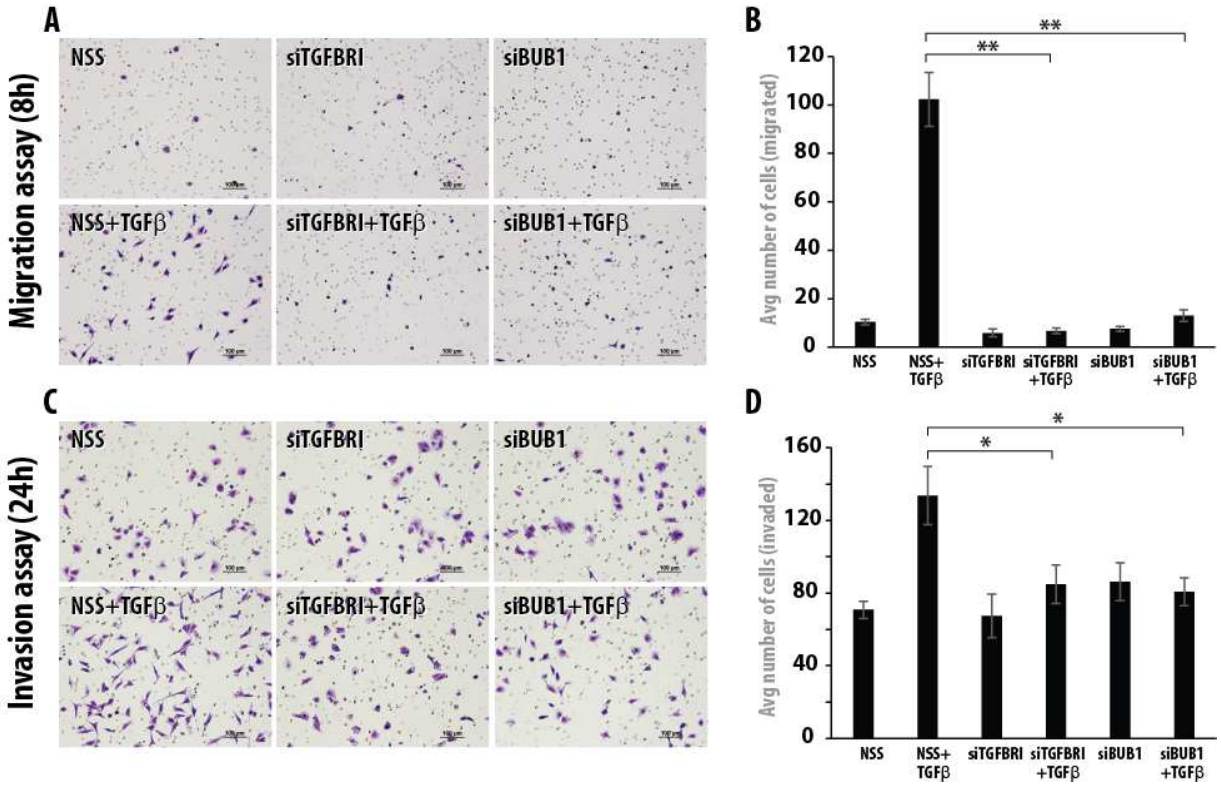

Figure S6. Depletion of BUB1 inhibits TGF-β–mediated migration and invasion of A549 cells. (A to D) Migration assays using 0.8 μM filter wells (A and B) and invasion assays using Matrigel-coated wells (C and D) in A549 cells transfected as indicated with control (NSS) or targeted siRNA in the absence or presence of TGF-β (10 ng/mL) for 72 hours. Cell migration and invasion were counted from two random fields for each treatment. Data are means ± S.E. from 3 biological replicates. *P<0.001, **P<0.01, two-sided Student's *t*-test. Images are representative. Scale bars, 100 μM.

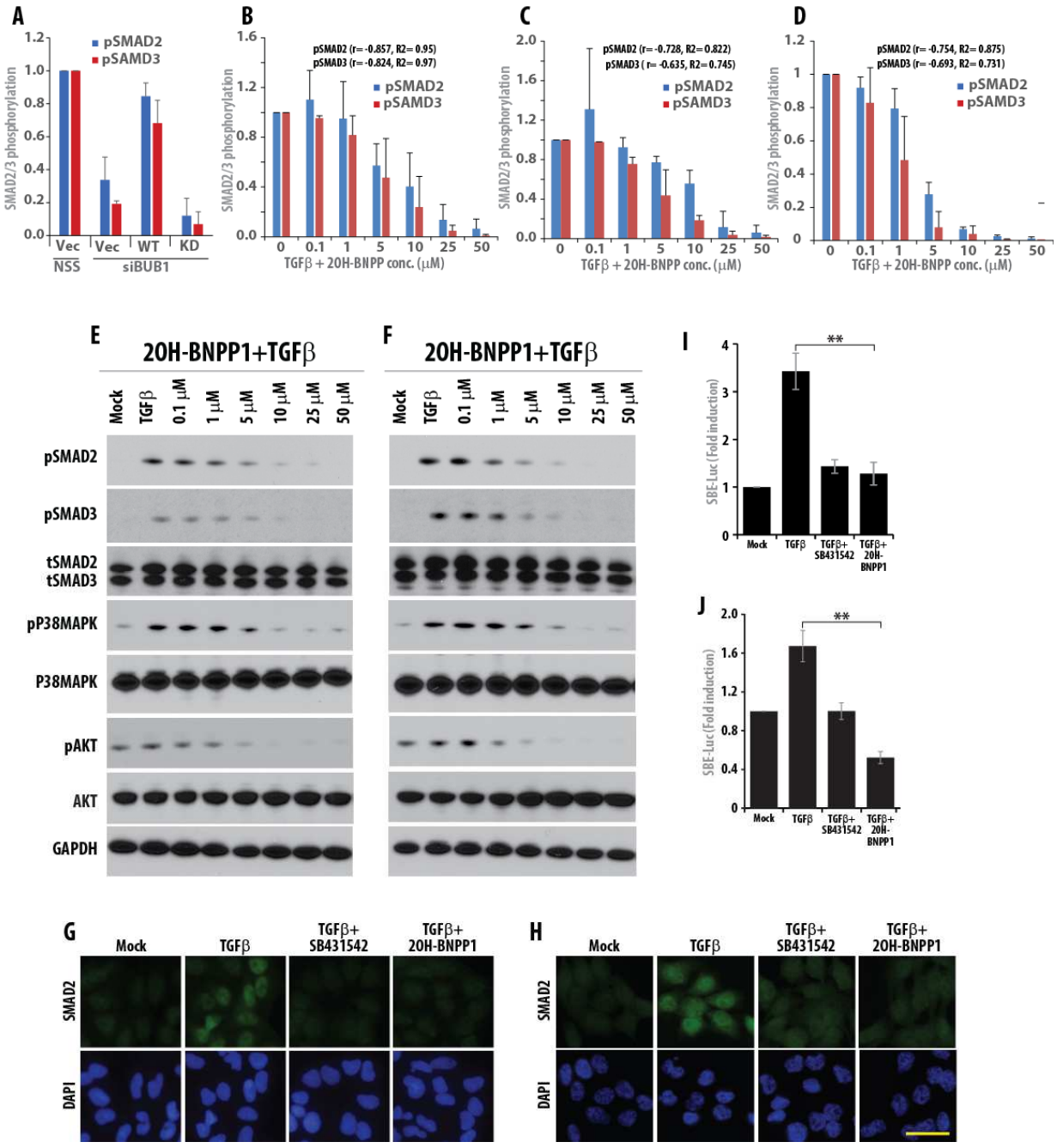

Figure S7. BUB1 kinase activity mediates TGF-β–dependent phosphorylation and nuclear activity of R-SMAD. (A) Quantitation of TGF-β-treated western blot data in Fig. 3A. Data are means ± S.E. from 2 biological replicates. **(B to D)** Quantitative analysis of immunoblot results in Fig. 3 (C to E). In A549 (B), NCI-H358 (**C**), and MDA-231-1833 (D) cells, pSMAD2/3 abundance and 2OH-BNPP1 concentration showed a strong negative correlation (r) and a strong goodness of fit (R^2). Data are means ± S.D. of 3 biological replicates for each cell lines. **(E and F)** Immunoblots of lysates from Het1A (E) and MRC5 (F) cells treated with vehicle, vehicle and TGF-β (10 ng/mL), or TGF-β and the indicated concentration of 2OH-BNPP1 for 1 hour. **(G and H)** Immunofluorescence analysis of SMAD2 in A549 (**G**) and NCI-H358 (**H**) cells treated with vehicle (mock), vehicle and TGF-β (10 ng/mL), or TGF-β and either SB-431542 (10 μM) or 2OH-BNPP1 (10 μM) for 1 hour. Nuclei were counter-stained with DAPI. Data are representative of 3 biological replicates. Scale bar, 25μm. **(I and J)** Relative firefly luciferase activity (normalized to Gaussia luciferase) in MDA-231-1833 (**I**) and HeLa (**J**) cells transiently transfected with the SBE4-Luc reporter plasmid and a GLuc plasmid and treated as in (G and H) for 24 hours. Data are means ± S.E.M. of 3 biological replicates. **P<0.001, two-sided Student's *t*-test.

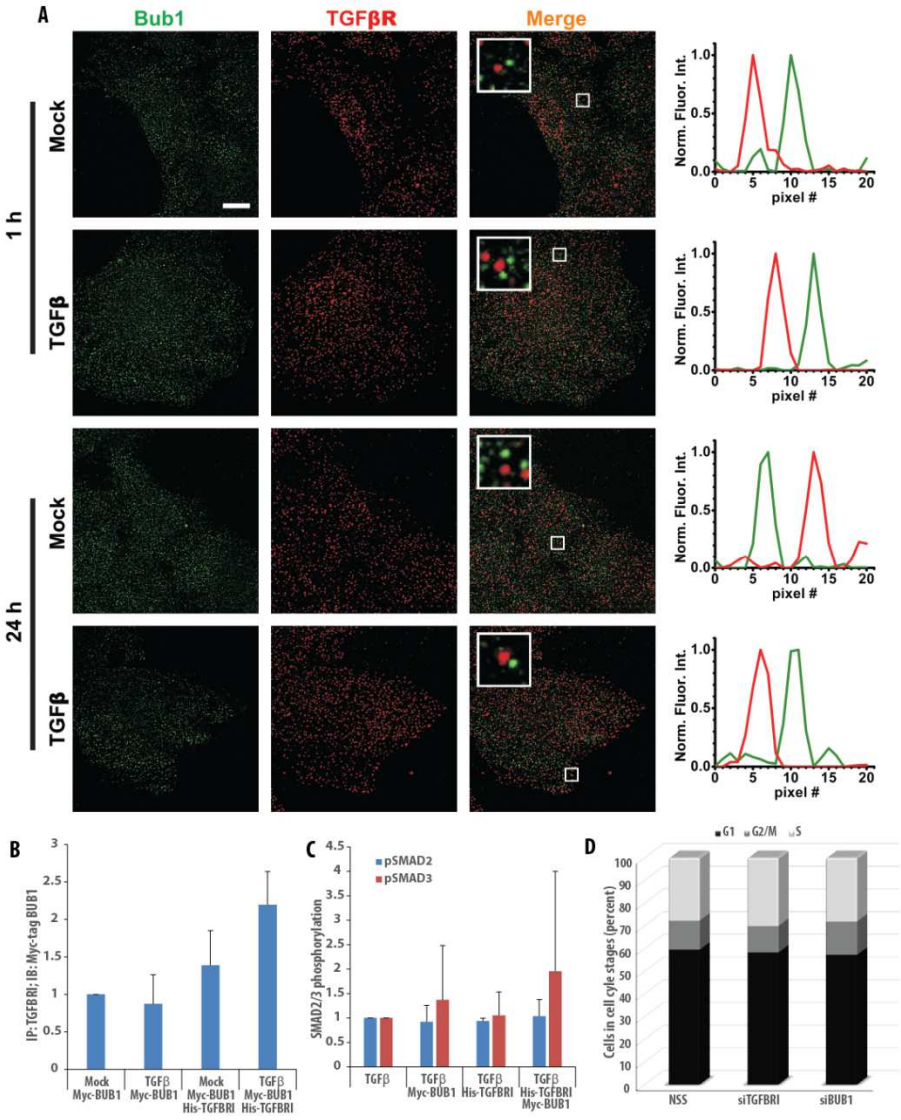

Figure S8. TGFBRI and BUB1 colocalization by TIRF microscopy at 1 and 24 hours and coimmonoprecipitation of His-TGFBRI and Myc-BUB1. (A) Pseudocolored, background-corrected, TIRF images of A549 cells that were treated with a mock reagent (top panel) or TGF-β (10 ng/mL, bottom panel) for 1 or 24 hours and immunostained for BUB1 (green) and TGFBRI (red). Scale bar, 10 µm. Insets ($2.66 \times 2.66 \mu m^2$) re magnified images of the boxed regions. Line scan across BUB1 (green) and TGFBRI (red) particles within the inset are shown at the right**.** Data are representative of 3 experiments. **(B and C)** Quantitation of immunoblotting represented in Fig. 4D: coimmunoprecipitation of Myc-BUB1 with TGFBRI (B), or abundance of phosphorylated SMAD2 or phosphorylated SMAD3 (C). Data are means ± S.E. of 3 experiments. **(D)** Cell cycle analysis by propidium iodide staining in A549 cells transfected with control siRNA (NSS), TGFBRI siRNA, or BUB1 siRNA for 72 hours. Combined data from 3 biological replicates is shown.

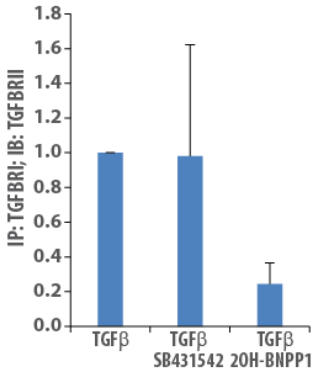

Figure S9. BUB1 kinase activity mediates TGFBRI-TGFBRII interaction. Quantitation of Western blotting data in Fig. 4G. Data are means ± S.E. from 3 experiments.

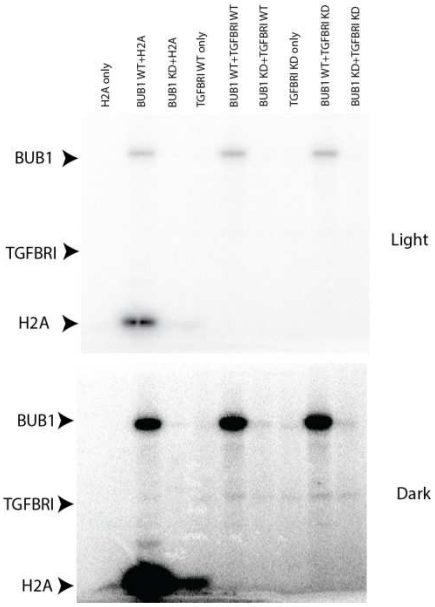

Figure S10. TGFBRI is not a direct substrate of BUB1 kinase activity. In vitro kinase assay containing varying combinations of insect cell-purified full-length wild-type (WT) or kinase-deficient (KD) BUB1 and full-length wild-type or kinase-deficient (KD) TGFBRI. H2A was used as a positive control. Data are representative of 3 experiments.

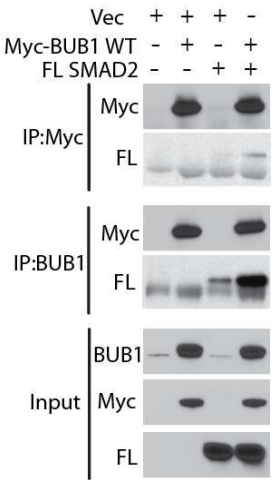

Figure S11. Wild-type Myc-BUB1 interacts with FL-SMAD2 in HEK293T cells. Immunoprecipitation for Myc or BUB1 from lysates of HEK293T cells transfected with wild-type Myc-BUB1 and Flag-tagged (FL) SMAD2. Input lysates were probed with control antibodies. Blots are representative of 2 experiments.

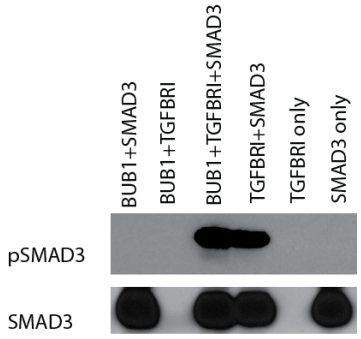

Figure S12. SMAD3 is not a direct substrate of BUB1 kinase activity. In vitro kinase assay containing varying combinations of insect cell-purified full-length wild-type BUB1 or TGFBRI and *E. coli*–purified GST-tagged SMAD3. Data are representative of 3 experiments.

Table S1. Human kinome siRNA screen in A549-BTR and MDA-231-1833–BTR cells. (Table is supplied as an Excel file in additional supplementary files online). BTR-fold change over non-targeting scrambled control (NSS) siRNA transfected cells is calculated for each replicate for each cell-line. Average of three replicates is calculated and the data is sorted based on the average reporter fold induction over control. Plate number for siRNA to specific kinase is provided in the first column. The data is deposited at PubChem (https://pubchem.ncbi.nlm.nih.gov/assay/assay.cgi?aid=1117269), accession ID 1117269.

Table S2. Hits obtained in A549-BTR and MDA-231-1833–BTR human kinome screen. (Table is supplied as an Excel file in additional supplementary files online). Hits obtained in A549-BTR (green) and MDA-231-1833-BTR (red). High stringency hits in experiment-wise analysis are shown in bold while low-stringency hits are in normal text. A reference for known association of a kinase with TGF-β signaling pathway is provided.

Table S3. Pathway impact analysis based on the fold induction of the BTR reporter. (Table is on the next page, below). Low and high-stringency hits (listed in table S2) were subjected to Pathway Impact Analysis. Rank, name, pathway ID, pathway size (pSize), number of differentially expressed genes (NDE, genes subjected to analysis), total perturbation accumulation (tA), p-values for over representation of differentially expressed genes in a given pathway ($P_{NDE,}$), the degree of perturbation (P_{PERT}), overall p-value (pG, combining P_{NDE} and P_{PERT}), overall FDR corrected p-value (pGFDR), overall FWER corrected p-value (pG FWER) are given.

Table S3. Pathway impact analysis based on the fold induction of the BTR reporter.

Rank	Pathway (A549-BTR)	Pathway ID	pSize	NDE	tA	pNDE	pPERT	pG	pG FDR	pG FWER
1	Insulin signaling pathway	4910	138	7	-4E+01	4E-12	0.35	4.06E-11	2.97E-09	2.97E-09
2	mTOR signaling pathway	4150	64	4	-2E+01	1E-07	0.085	1.65E-07	6.00E-06	1.20E-05
3	Adipocytokine signaling pathwa	4920	69	4	-6E+00	1E-07	0.647	1.50E-06	2.99E-05	1.09E-04
4	ErbB signaling pathway	4012	88	4	-4E+01	4E-07	0.266	1.64E-06	2.99E-05	1.20E-04
5	MAPK signaling pathway	4010	259	5	-2E+01	8E-07	0.178	2.29E-06	3.34E-05	1.67E-04
6	Progesterone-mediated oocyte maturation	4914	86	4	4E-01	3E-07	0.939	4.91E-06	5.97E-05	3.58E-04
7	Neurotrophin signaling pathway	4722	120	4	-9E+00	1E-06	0.51	9.69E-06	1.01E-04	7.07E-04
8	Type II diabetes mellitus	4930	48	3	-8E+00	5E-06	0.709	4.38E-05	4.00E-04	3.20E-03
9	Toxoplasmosis	5145	118	3	3E+01	7E-05	0.068	6.12E-05	4.96E-04	4.47E-03
10	Influenza A	5164	174	3	3E+01	2E-04	0.032	8.81E-05	6.43E-04	6.43E-03
11	Fc gamma R-mediated phagocytos	4666	95	3	-9E+00	4E-05	0.341	1.49E-04	9.89E-04	1.09E-02
12	Phosphatidylinositol signaling	4070	81	3	8E-17	2E-05	0.991	2.56E-04	1.56E-03	1.87E-02
13	Tuberculosis	5152	179	3	4E+01	2E-04	0.111	2.98E-04	1.67E-03	2.17E-02
14	HIF-1 signaling pathway	4066	110	3	4E+00	5E-05	0.658	4.06E-04	2.12E-03	2.96E-02
15	PI3K-Akt signaling pathway	4151	338	4	2E+01	7E-05	0.632	5.08E-04	2.47E-03	3.71E-02

16	Chemokine signaling pathway	4062	189	3	2E+01	3E-04	0.417	1.14E-03	5.22E-03	8.35E-02
17	Focal adhesion	4510	204	3	-2E+01	3E-04	0.42	1.41E-03	5.87E-03	1.03E-01
18	Bacterial invasion of epitheli	5100	70	2	4E+01	1E-03	0.146	1.45E-03	5.87E-03	1.06E-01
19	Circadian rhythm	4710	30	2	8E-01	2E-04	0.969	1.72E-03	6.63E-03	1.26E-01
20	Cholinergic synapse	4725	112	2	6E+01	3E-03	0.076	1.85E-03	6.76E-03	1.35E-01
31	Oocyte meiosis	4114	112	2	3E+01	3E-03	0.428	8.55E-03	2.01E-02	6.24E-01
32	**TGF-beta signaling pathway**	4350	83	2	-6E-14	1E-03	0.836	9.15E-03	2.09E-02	6.68E-01

Rank	Pathway (MDA-231-1833 BTR)	Pathway ID	pSize	NDE	tA	pNDE	pPERT	pG	pG FDR	pG FWER
1	**TGF-beta signaling pathway**	4350	83	3	-7E+01	2E-05	0.309	9.38E-05	6.76E-03	6.76E-03
2	ErbB signaling pathway	4012	88	3	3E+01	3E-05	0.773	2.56E-04	9.21E-03	1.84E-02
3	mTOR signaling pathway	4150	64	2	-4E+01	8E-04	0.063	5.77E-04	1.38E-02	4.15E-02
4	Phototransduction	4744	29	1	-1E+02	2E-02	0.005	9.83E-04	1.77E-02	7.08E-02
5	Phosphatidylinositol signaling	4070	81	2	1E+01	1E-03	0.101	1.35E-03	1.80E-02	9.71E-02
6	Chemokine signaling pathway	4062	189	3	-5E+01	3E-04	0.565	1.50E-03	1.80E-02	1.08E-01
7	Leishmaniasis	5140	72	2	3E+01	1E-03	0.256	2.52E-03	2.42E-02	1.81E-01
8	Acute myeloid leukemia	5221	57	2	-1E+01	7E-04	0.439	2.69E-03	2.42E-02	1.94E-01
9	Progesterone-mediated oocyte maturation	4914	86	2	3E+01	2E-03	0.351	4.55E-03	3.47E-02	3.27E-01

10	Toxoplasmosis	5145	118	2	4E+01	3E-03	0.211	5.03E-03	3.47E-02	3.62E-01
11	HIF-1 signaling pathway	4066	110	2	2E+01	2E-03	0.258	5.32E-03	3.47E-02	3.83E-01
12	Influenza A	5164	174	2	4E+01	6E-03	0.116	5.78E-03	3.47E-02	4.16E-01
13	Herpes simplex infection	5168	184	2	3E+01	7E-03	0.118	6.45E-03	3.57E-02	4.64E-01
14	Oocyte meiosis	4114	112	2	8E+01	3E-03	0.348	7.13E-03	3.67E-02	5.14E-01
15	Cholinergic synapse	4725	112	2	6E+01	3E-03	0.408	8.20E-03	3.93E-02	5.90E-01
16	Dorso-ventral axis formation	4320	24	1	-1E+01	2E-02	0.072	8.90E-03	4.00E-02	6.41E-01
17	PI3K-Akt signaling pathway	4151	338	3	2E+00	1E-03	0.985	1.09E-02	4.61E-02	7.84E-01
18	Insulin signaling pathway	4910	138	2	3E+01	4E-03	0.437	1.24E-02	4.84E-02	8.93E-01
19	Fc gamma R-mediated phagocytos	4666	95	2	1E+00	2E-03	0.939	1.28E-02	4.84E-02	9.19E-01
20	Tuberculosis	5152	179	2	5E+01	6E-03	0.306	1.41E-02	5.08E-02	1.00E+00